A Vibrating Barrier With Grounded Inerter For Non-Invasive Seismic Protection Of Existing Structures

Pierfrancesco CACCIOLA[1], Alessandro TOMBARI[2], Agathoklis GIARALIS[3]

ABSTRACT

The recently proposed by the first two authors Vibrating Barrier (ViBa) can be interpreted as a large-scale linear mass-damper unit buried in the ground and tuned/designed to protect surrounding structures without being directly in contact to them through a structure-soil-structure interaction mechanism. Previous research demonstrated that ViBa achieves significant structural response reduction at a cost of excessive required vibrating mass of the order of the mass of the structure sought to protect. To this end, this paper considers coupling ViBa with a grounded inerter device acting as a mass amplifier to reduce the required mass/weight of ViBa in suppressing seismically induced vibrations in structures amenable to modelling as single-degree-of freedom (SDOF) damped oscillators. The equations of motion and transfer function of a grounded inerter ViBa (IViBa) fused with a SDOF structure are derived. Two different optimal design approaches are discussed to tune the IViBa to minimize the displacement response of SDOF structure subject to harmonic and to broadband base excitations in the H_∞ and H_2 optimal control context. Pertinent numerical results are furnished associated with the properties of a small-scale ViBa prototype specimen to quantify the effect of the grounded inerter of different inertial property to the vibration control performance of optimally tuned IViBa. It is shown numerically using both H_2 optimal performance results as well as response history analyses for an artificial quasi-stationary accelerogram that IViBa mass/weight can effectively be traded for grounded inerter inertial property to achieve the same level of structural vibration suppression to broadband seismic excitation.

Keywords: Vibrating Barrier; inerter; structure-soil-structure interaction; optimal design

[1]Principal Lecturer, University of Brighton, Brighton, UK, P.Cacciola@brighton.ac.uk
[2]Lecturer, University of Brighton, Brighton, UK, A.Tombari@brighton.ac.uk
[3]Senior Lecturer, Dept. Civil Engineering, City, University of London, London, UK, agathoklis@city.ac.uk

1. INTRODUCTION

Seismic protection of new buildings is commonly addressed through ductile design for earthquake resistance (e.g., Avramidis et al. 2016) or by using supplemental damping devices (Soong and Dargush 1997) and/or base isolation systems (e.g., Naeim and Kelly 1999). Nevertheless, the seismic protection of existing code-deficient buildings and heritage structures is an appreciably more involved task from the engineering as well as the architectural viewpoint requiring obtrusive and expensive structural intervention. Moreover, as evidenced by recent earthquakes, such as the 2016 event in Amatrice, Italy, increasing the resilience of entire communities living in rather vulnerable structures to seismic hazard in a cost-effective manner is a timely issue and an open challenge.

In addressing the above needs and challenges in an efficient manner, a novel passive control solution termed Vibrating Barrier (ViBa) has been recently proposed by Cacciola and Tombari (2015). ViBa comprises a free-to-vibrate mass encased in a rigid box buried in the ground and connected to the walls of the box through linear springs and dampers. It can therefore be viewed as a contained underground tuned mass-damper (TMD) unit designed/tuned to damp out portion of the seismic energy before entering the foundations of surrounding structures by exploiting a structure-soil-structure (SSSI) mechanism. To date, several studies on the efficiency of the ViBa has been carried out to mitigate the seismic vulnerability of different structures. Cacciola et al. (2015) investigated the potential of ViBa for the seismic protection of monopiled structures, Tombari et al. (2016) considered ViBa to mitigate seismic risk of a nuclear reactor, Cacciola et al. (2017) applied ViBa to control the seismic response of a heritage building, while the ViBa technology was used to protect a large urban area in Coronado et al. (2017), as well as a cluster of buildings in Tombari et al. (2018). All the above studies have collectively demonstrated the high efficiency of ViBa in reducing peak structural response which, in the case of narrow-band/harmonic excitations, can be higher than 60%, while for broadband/earthquake excitations reaches more than 30%. Nevertheless, the effectiveness of ViBa in containing structural

seismic response demands depends largely on its inertial property: the higher the ViBa mass is, the more dramatic the reductions in peak structural response becomes. In this regard, the above reported reductions to seismic response require a ViBa mass as large as the total mass of the structure to be protected which needs to be embedded to the ground. This requirement results in significant excavation, underground space usage, and construction costs which reduces the applicability of ViBa in real-life applications.

In this regard, this paper aims to address the drawback of excessive required ViBa mass by incorporating a grounded inerter device to the ViBa acting as a mass amplifier (Smith 2002). This consideration is motivated by the work of Marian and Giaralis (2014 and 2017) who showed that the inclusion of a grounded inerter to the classical TMD results in significant TMD mass/weight reduction for fixed vibration suppression performance in terms of host structure peak displacement for stochastic wide-band (white) and harmonic base excitations, respectively. Herein, the inerter is taken as a two-terminal mechanical element developing a resisting force proportional to the relative acceleration of its terminals (Smith 2002). The inerter constant of proportionality is termed inertance and is measured in mass (kg) units. Theoretically, the inertance is independent of the mass/weight of the inerter device. Indeed, inerter device prototypes have been manufactured and tested/verified experimentally attaining inertances several orders of magnitude larger than their physical mass (e.g. Papageorgiou and Smith 2005, Watanabe et al. 2012).

In what follows, a linear mechanical model of a ViBa with grounded inerter is proposed in Section 2 to reduce seismic demands in a single neighboring structure represented by means of a SDOF system. The governing equations of motion and frequency domain transfer function matrix are derived. Next, two different optimal design approaches, one pertinent to harmonic ground excitation and one suited for broad-band ground excitation, for the tuning of the proposed device to minimize structural response displacement are discussed in Section 3. The performance of several different optimally designed ViBa with grounded inerter is numerically assessed in Section 4 focusing on appraising the different optimal tuning approaches for earthquake excitations and on quantifying ViBa mass/weight reduction achieved

by the grounded inerter for fixed vibration suppression performance. Lastly, Section 5 summarizes the main conclusions.

2. THE VIBRATING BARRIER WITH GROUNDED INERTER

2.1 Mechanical model description

Consider a planar structure represented by a linear viscously damped single-degree-of-freedom (SDOF) system with stiffness *k,* damping coefficient *c,* and mass *m* resting on compliant soil. The structure is subjected to earthquake-induced horizontal ground displacement, u_g, and a ViBa incorporating an ideal inerter device, hereafter termed IViBa, is used to mitigate the structure oscillatory motion through a SSSI mechanism [see Cacciola and Tombari (2015) and references therein for further details on SSSI phenomena]. Shown in Figure 1 is a linear discrete mechanical model of an IViBa fused with the SDOF structural system put forward in this work to examine the effectiveness of the IViBa for seismic protection of structures. In the model, soil-structure interaction (SSI) effects to structural response due to soil compliance of the supporting ground are accounted for through the stiffness, k_f, damping coefficient, c_f, and lumped foundation mass, m_f. Further, the IViBa is represented by an internal linear SDOF oscillating unit with lumped mass, m_{IViBa}, spring stiffness, k_{IViBa} , and damping coefficient, c_{IViBa} as well as of an external containment with lumped mass $m_{f,IViBa}$ (Cacciola and Tombari 2015). An inerter element with inertance b connects the IViBa oscillating unit to the ground. The SSI effects associated with the IViBa are modelled through the stiffness coefficient, $k_{f,IViBa}$ and the damping coefficient $c_{f,IViBa}$. Lastly, the SSSI mechanism is modelled using a linear elastic spring with k_{SSSI} stiffness constant and a dashpot with c_{SSSI} damping coefficient linking the foundation of the SDOF structure to the IViBa.

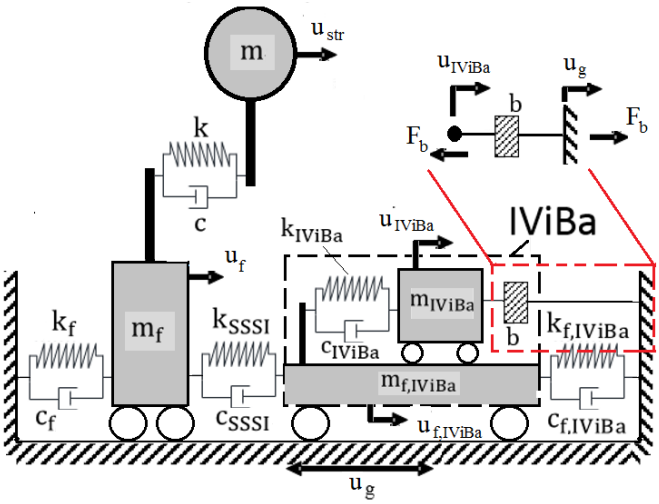

Figure 1. Mechanical model of an IViBa used to protect a linear SDOF structure.

Compared to the original ViBa configuration and its underlying dynamical model introduced in Cacciola and Tombari (2015), the key additional component furnished by the IViBa is the inerter element with one terminal grounded indicated by a red box in Figure 1. In the herein proposed IViBa configuration, the inerter develops a resisting force $F_b = b(\ddot{u}_{IViBa} - \ddot{u}_g)$, shown in the inlet of Figure 1 under the assumption of $\ddot{u}_{IViBa} > \ddot{u}_g$, where u_{IViBa} is the absolute displacement of the IViBa oscillating unit and hereafter a dot over a symbol denotes differentiation with respect to time. This force is added to the IViBa mass (inertial) force, $m_{IViBa}\ddot{u}_{IViBa}$ and, therefore, the inertance property of the grounded inerter contributes to the overall inertia of the IViBa unit. Nevertheless, similarly to dashpots representing linear viscous damping devices, the inerter is taken as mass-less since the inertance b can be several orders of magnitude larger than the physical device mass (see e.g., Smith 2002, Watanabe et al. 2012, Marian and Giaralis 2017). In this respect, the grounded inerter acts as an apparent mass amplifier since it adds to the inertial property or, equivalently, to the inertial resisting force of the IViBa without increasing the IViBa weight. Clearly, for b=0, the inerter contributing force becomes zero (i.e., $F_b = 0$) and the IViBa degenerates to the original ViBa.

2.2 Equations of motion in frequency domain and transfer function vector

The motion of the seismically excited mechanical model in Figure 1 can be described by 4 degrees-of-freedom (DOFs) taken here to be the absolute displacements of the SDOF structure and its foundation, u_{str} and u_f, respectively, as well as the absolute displacements of the IViBa oscillating unit and its containment, u_{IViBa} and $u_{f,IViBa}$, respectively, as noted on Figure 1. The equations of motion can be written in the domain of circular frequency ω as

$$[\mathbf{K} - \omega^2\mathbf{M} + i\omega\mathbf{C}]\mathbf{U}(\omega) = \mathbf{Q}\, U_g(\omega) \tag{1}$$

in which $i = \sqrt{-1}$; $U_g(\omega)$ is the Fourier transform of the ground displacement; $\mathbf{U}(\omega)$ is the vector collecting displacements along the 4 DOFs of the system upon Fourier transformation written as

$$\mathbf{U}^T(\omega) = [U_{str}(\omega) \quad U_f(\omega) \quad U_{IViBa}(\omega) \quad U_{f,IViBa}(\omega)] \tag{2}$$

where the superscript "T" is the matrix transpose operator; $\mathbf{Q}$ is the influence vector defined as

$$\mathbf{Q}^T = [0 \quad k_f + i\omega c_f \quad -\omega^2 \quad k_{f,IViBa} + i\omega c_{f,IViBa}] \tag{3}$$

and the inertial (mass and inertance) matrix $\mathbf{M}$, stiffness matrix $\mathbf{K}$, and damping matrix $\mathbf{C}$ are given as

$$\mathbf{M} = \begin{bmatrix} m & 0 & 0 & 0 \\ 0 & m_f & 0 & 0 \\ 0 & 0 & m_{IViBa} + b & 0 \\ 0 & 0 & 0 & m_{f,IViBa} \end{bmatrix},$$

$$\mathbf{K} = \begin{bmatrix} k & -k & 0 & 0 \\ -k & k + k_f + k_{SSSI} & 0 & -k_{SSSI} \\ 0 & 0 & k_{IViBa} & -k_{IViBa} \\ 0 & -k_{SSSI} & -k_{ViBa} & k_{IViBa} + k_{f,IViBa} + k_{SSSI} \end{bmatrix}, \text{and} \quad (1)$$

$$\mathbf{C} = \begin{bmatrix} c & -c & 0 & 0 \\ -c & c + c_f + c_{SSSI} & 0 & -c_{SSSI} \\ 0 & 0 & c_{IViBa} & -c_{IViBa} \\ 0 & -c_{SSSI} & -c_{IViBa} & c_{IViBa} + c_{f,IViBa} + c_{SSSI} \end{bmatrix},$$

respectively. The transfer function vector of the 4-DOF system in Figure 1 is given by

$$\mathbf{H}(\omega) = \mathbf{K}_{dyn}^{-1}(\omega)\mathbf{Q} = [H_{str}(\omega) \quad H_f(\omega) \quad H_{IViBa}(\omega) \quad H_{f,IViBa}(\omega)]^T \quad (5)$$

where $\mathbf{K}_{dyn}(\omega) = \mathbf{K} - \omega^2\mathbf{M} + i\omega\mathbf{C}$ is the dynamic stiffness matrix and the superscript "-1" denotes matrix inversion. The first element of the transfer function vector in Equation 5, i.e., the transfer function $H_{str}(\omega)$ corresponding to the SDOF system displacement, forms the basis for optimal tuning/designing of the IViBa for harmonic and for broad-band excitations discussed in the following section. It is further reiterated that for b=0 the equations of motion in Equation 1 and the transfer function vector in Equation 5 correspond to the original ViBa (Cacciola and Tombari 2015).

3. OPTIMAL DESIGN OF VIBA WITH GROUNDED INERTER

3.1 Design variables

In minimizing the displacement response u_{str} of a given structure to known seismic excitation in Figure 1, the properties $k_{IViBa}, m_{IViBa}, c_{IViBa}$, and b of the IViBa become the unknown parameters of the underlying optimization problem. This is because foundation and SSI related parameters can be taken

as known; determined through foundation and geotechnical design involving the geometry of the structure foundation and of the IViBa containment as well as of the soil properties. Moreover, Cacciola et al. (2015) demonstrated that ViBa efficiency for seismic vibrations mitigation increases with increasing the mass of the ViBa oscillating unit. Therefore, mass, m_{IViBa}, and inertance, b, are herein specified *a priori*. In this setting, optimal IViBa design involves determining two design variables, namely the stiffness, k_{IViBa}, and the viscous damping coefficient, c_{IViBa}, such that the internal IViBa oscillator unit with given inertial properties m_{IViBa} and b is optimally "tuned" to minimize the peak displacement u_{str} of a given structure subjected to known seismic excitation. The two design variables are collected in the design parameters vector $\boldsymbol{\alpha} = [k_{IViBa}, c_{IViBa}]^T$.

3.2 Optimal H_∞ design for harmonic excitation

Consider first the case of harmonic ground excitation in which $U_g(\omega_f) = 1$ in Equation 1 where ω_f is the circular frequency of the excitation. Minimization of peak u_{str} can be achieved by requiring that the magnitude of the transfer function $H_{str}(\omega)$ in Equation 5 at $\omega = \omega_f$ is minimized through optimal IViBa tuning. The above optimization problem can be mathematically expressed as

$$\min_{\boldsymbol{\alpha}}\{|H_{str}(\omega_f)|\} \text{ where } \boldsymbol{\alpha} = \{k_{IViBa}, c_{IViBa}\} \in \mathbb{R}_0^+ \tag{6}$$

supporting optimal control design in the infinity norm H_∞ sense (see e.g. Zuo, 2009; Toscano, 2013). It can be solved in closed-form by finding the zeros of the transfer function $H_{str}(\omega)$ at frequency ω_f. After some algebra, the following formula is derived

$$\bar{k}_{IViBa} = \frac{m_{IViBa}\cdot\omega_f^2(\mu+1)\left[\bar{k}_{sssi}+\chi\cdot(\bar{k}_f+\bar{k}_{sssi})-m_{fv}\cdot\omega_f^2\right]}{\chi(\bar{k}_{sssi}+\bar{k}_f)+\bar{k}_{sssi}-\omega_f^2\left(m_{fv}-m_{IViBa}(\mu+1)-\mu\cdot\bar{k}_{sssi}/\bar{k}_f\cdot m_{IViBa}\right)} \tag{7}$$

where

$$\mu = \frac{b}{m_{IViBa}} \text{ and } \chi = \frac{\bar{k}_{f,IViBa}}{\bar{k}_f} \tag{8}$$

and $\bar{k}_x$ denotes the complex quantity $k_x + i\omega_f c_x$. The optimal tuning parameters of the IViBa under harmonic excitation are obtained as

$$k_{IViBa} = \Re\{\bar{k}_{IViBa}\} \; and \; c_{IViBa} = \frac{\Im\{\bar{k}_{IViBa}\}}{\omega_f} \tag{9}$$

where $\Re\{\bar{k}_{IViBa}\}$ and $\Im\{\bar{k}_{IViBa}\}$ are the real and imaginary parts of $\bar{k}_{IViBa}$ in Equation 7, respectively.

3.3 Optimal H_2 design for broad-band (white noise) excitation

In case of broad-band excitation $U_g(\omega)$, minimization of peak u_{str} can be achieved by minimizing the second (i.e., L_2) norm of $H_{str}(\omega)$ leading to a H_2 optimal control design (e.g. Zuo, 2009, Toscano 2013). That is,

$$\min_{\boldsymbol{\alpha}}\{\|H_{str}(\omega)\|^2\} \text{ where } \boldsymbol{\alpha} = \{k_{IViBa}, c_{IViBa}\} \in \mathbb{R}_0^+ \tag{10}$$

in which $\|H_{str}(\omega)\|^2 = \int_0^{\omega_{cut}} H_{str}^*(\omega)\, H_{str}(\omega) d\omega$ where $H_{str}^*(\omega)$ is the conjugate of $H_{str}(\omega)$ and ω_{cut} is a frequency value above which the integrand takes on negligible values. The above optimal tuning of the IViBa ensures that the displacement response variance of the structure is minimized under white noise ground excitation and, therefore, so does the peak u_{str} response. In the ensuing numerical work, the default pattern search algorithm of MATLAB® is used to solve the minimization problem in Equation 10 numerically.

4. NUMERICAL RESULTS

This section furnishes and discusses numerical results quantifying the effectiveness of H_∞ and H_2 optimally tuned IViBa with different mass and inertance properties to reduce seismic displacement demands of the SDOF structural system in Figure 1. The presentation begins by describing a benchmark mechanical model of Figure 1 used in all subsequent numerical work derived from a small-scale prototype specimen.

4.1 Adopted benchmark model of a small-scale prototype specimen

Putting aside the IViBa properties $k_{IViBa}, m_{IViBa}, c_{IViBa}$, and b, the set of the remaining properties of the mechanical model in Figure 1 listed in Table 1 is used in the numerical part of this study. These properties are derived from a physical small-scale ViBa prototype specimen used to control the response of a SDOF structure presented in detail in Cacciola and Tombari (2015). The various mass and stiffness properties are extracted directly from the manufactured prototype. The viscous damping coefficients are computed from the corresponding non-dimensional loss factor, η, values used in Cacciola and Tombari (2015) by means of the expression

$$c = \frac{\eta \cdot k}{\omega_0} \tag{11}$$

where $\omega_0 = 22.62$ rad/s is the fundamental natural frequency of the SDOF structure accounting for soil compliance at its foundation. Note that Equation 11 is strictly valid for harmonic input only and maps a hysteretic type of damping, widely used in SSI studies, according to which the complex impedance is given as $k(1 + i\eta)$, by a viscous type of damping in which complex impedance is defined as $k + i\omega_0 c$.

Table 1. Adopted mechanical properties for the model in Figure 1 corresponding to the small-scale prototype

specimen in Cacciola and Tombari (2015).

Property	**SDOF structure**	**SSI (structure)**	**SSI (IViBa)**	**SSSI**
mass	m= 0.590 kg	m_f= 0.353 kg	$m_{f,IViBa}$= 0.491 kg	-
stiffness	k= 909.85 N/m	k_f= 640 N/m	$k_{f,IViBa}$= 760 N/m	k_{SSSI}= 315 N/m
loss factor	η= 0.1	η_f= 0.1	$\eta_{f,IViBa}$= 0.1	η_{SSSI}= 0.02
damping coefficient	c= 4.000 Ns/m	c_f= 2.814 Ns/m	$c_{f,IViBa}$= 3.341 Ns/m	c_{SSSI}= 0.277 Ns/m

4.2 Optimal H_∞ IViBa tuning for harmonic base excitation

The problem of minimizing the steady state response of the SDOF structure in Figure 1 for the properties of Table 1 is herein considered for harmonic ground excitation (i.e., $U_g(\omega_f) = 1$) with frequency equal to the natural frequency of the SDOF structure with flexible basis (i.e., $\omega_f = \omega_0 = 22.62$ rad/s). To this aim, the optimization problem in Equation 6 is solved to determine optimal positive IViBa stiffness, k_{IViBa}, and damping coefficient, c_{IViBa} for different values of IViBa mass, m_{IViBa}, and inertance, b. This is achieved by using Equations 7 to 9. The magnitude of the transfer function $H_{str}(\omega)$ in Equation 5 or the frequency response function (FRF) is used in assessing the performance of different optimal IViBa designs.

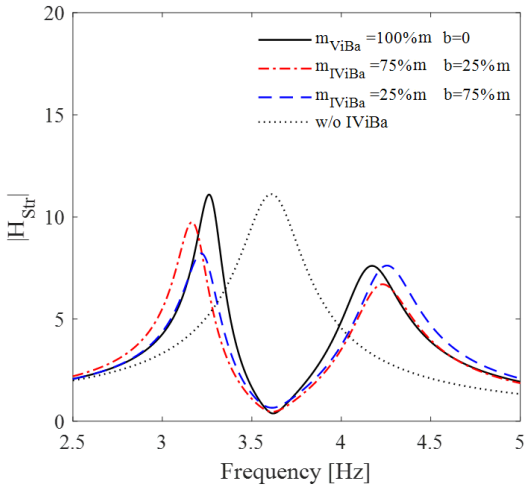

Figure 2. Frequency response function of H_∞ optimally designed IViBa for various mass and inertance values.

Figure 2 plots the $H_{str}(\omega)$ FRF for two optimal IViBa designs with total IViBa inertia (mass plus inertance) equal to the mass of the SDOF structure to be protected, i.e., $m_{IViBa} + b = m$. One design has a relatively large IViBa mass equal to 0.75m and small inertance equal to 0.25m, while the other design has a relatively small IViBa mass, 0.25m, and large inertance, 0.75m. On the same figure the FRF of a structure protected by an optimally designed ViBa (b=0) with $m_{IViBa} = m$ is also plotted as well as the FRF of the uncontrolled structure. It is seen that both IViBa designs achieve only slightly worse structural response reduction at the resonance frequency $\omega_f = \omega_0$ compared to the much heavier conventional ViBa. Specifically, the ViBa reduces steady-state structural response at resonance frequency by 97% compared to the uncontrolled structure, while a reduction of 96% and 94% is achieved for the IViBa with inertance $b = 0.25m$ and $b = 0.75m$, respectively. Therefore, for IViBa with equal total inertial property $m_{IViBa} + b$, slightly better performance at resonance frequency is achieved for larger mass and smaller inertance. Interestingly, IViBa with larger inertance reduces significantly the peak FRF value which is, however, attained at frequencies lower than the structural resonant frequency targeted by the herein considered H_∞ optimal control formulation.

Next, Figure 3 plots $H_{str}(\omega)$ FRFs of H_∞ optimally designed IViBa with fixed IViBa mass property equal to 0.5m (Figure 3a) and to m (Figure 3b) and for several inertance values. The FRF of a ViBa

with $m_{IViBa} = m$ is also plotted in the figures as well as the FRF of the uncontrolled structure. It is seen that the IViBa suppresses effectively the FRF ordinate at the excitation frequency, ω_o, targeted by the optimal control design by over 92% for all inertance values considered and for both m_{IviBa} values. It is further seen that the increase of inertance reduces significantly the value of the leftmost FRF lobe while it moves its location to lower frequencies (i.e., away from the resonant frequency). The increase of the inertance affects similarly the value and the location of the rightmost FRF lobe, though it is the m_{IViBa} property that mostly suppresses this second lobe.

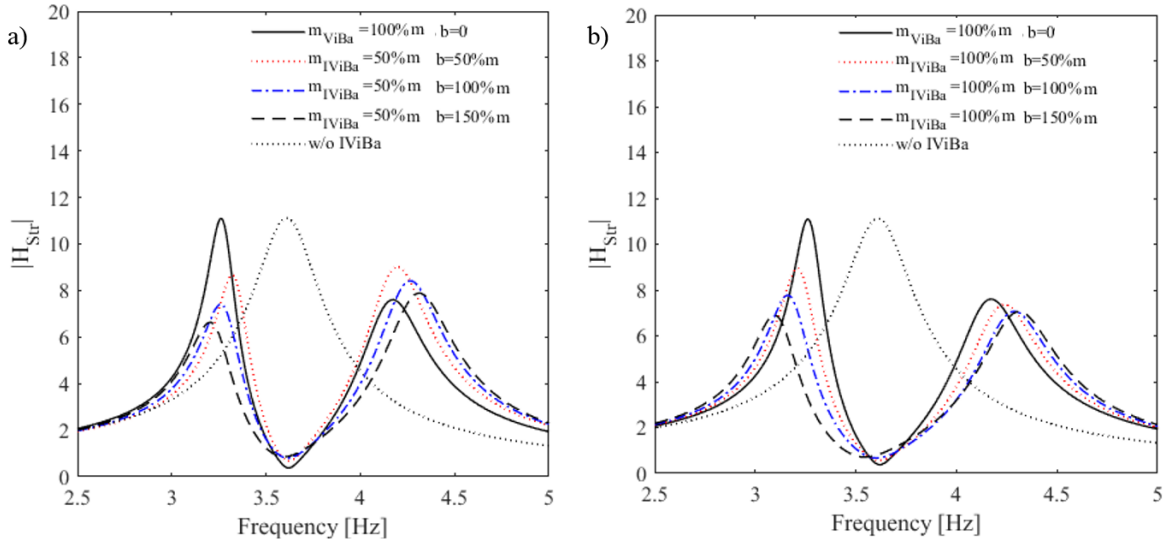

Figure 3. Frequency response function of H_∞ optimally designed IViBa for several values of inertance and for a) m_{IviBa}=0.5m, and b) m_{IviBa}=m.

4.3 Optimal H_2 IViBa tuning for broad-band excitation

This sub-section presents $H_{str}(\omega)$ FRFs for IViBa optimally designed to minimize the root-mean-square (RMS) displacement response of the SDOF structure in Figure 1 subject to broad-band (i.e., clipped white noise) stochastic excitation given as $U_g(\omega) = 1$ for $0 \leq \omega \leq \omega_{cut} = 31.42$ rad/s = 5 Hz. The same system properties of Table 1 are adopted as before and the optimization problem of Equation 10 is solved numerically to determine optimal IviBa stiffness, k_{IviBa}, and damping coefficient, c_{IviBa},

values for different values of IViBa mass, m_{IViBa}, and inertance, b.

Figure 4 plots the $H_{str}(\omega)$ FRF for the same IViBa cases shown in Figure 2 but now optimally designed in the H_2 sense aiming to minimize the area below the FRFs. It is seen that as the inertance increases for (I)ViBa with the same inertia, better vibration suppression in the RMS displacement is achieved.

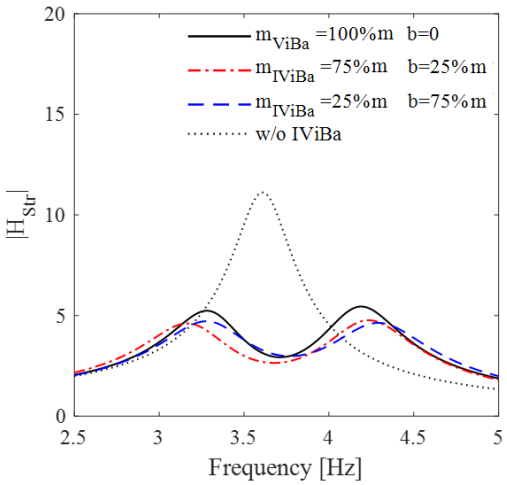

Figure 4. Frequency response function of H_2 optimally designed IViBa for various mass and inertance values.

Further, Figure 5 plots $H_{str}(\omega)$ FRFs of H_2 optimally designed IViBa with fixed IViBa mass property equal to 0.5m (Figure 5a) and to m (Figure 5b) and for several inertance values as in Figure 3. It is evidenced that the area below the FRF curves reduces with increasing inertance. For the relatively light IViBa (Figure 5a), larger reductions are observed around the second (rightmost) FRF lobe, while for the heavier IViBa (Figure 5b) the increase of inertance above m is locally detrimental around the second lobe, though still beneficial across the whole range of excitation frequencies.

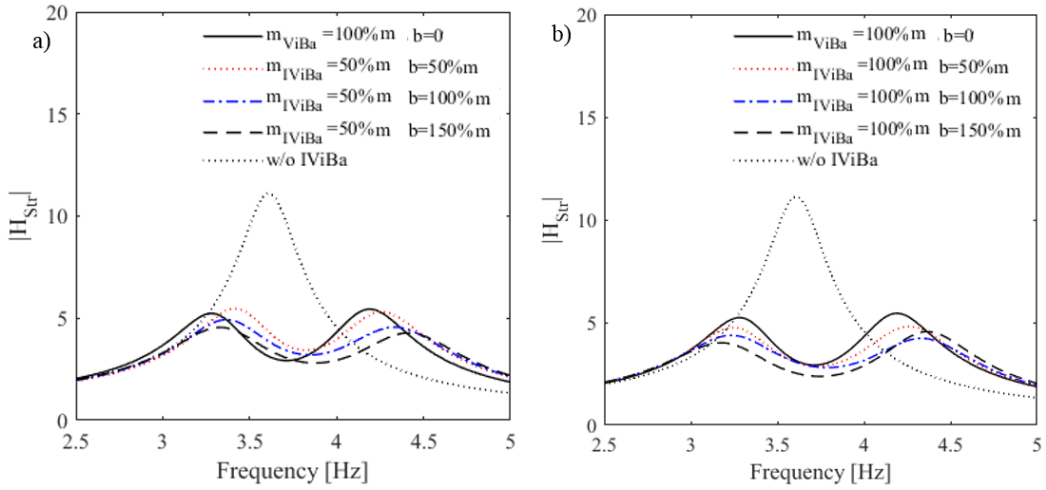

Figure 5 Frequency response function of H_2 optimally designed IViBa for several values of inertance and for a) m_{IviBa}=0.5m, and b) m_{IviBa}=m.

4.4 Comparison between H_∞ and H_2 optimal IViBa design and mass reduction quantification

The $H_{str}(\omega)$ FRFs obtained by IViBa optimally tuned to the two different design approaches discussed above are remarkably different. To facilitate a comparison, Figure 6a plots vis-à-vis $H_{str}(\omega)$ FRFs obtained by IViBa optimally designed in the H_∞ (tuned for harmonic excitation at the structural frequency) and H_2 (tuned for white noise excitation) sense with $m_{IViBa} = m$ and $b = 1.5m$. It is seen that H_∞ optimal tuning achieves significant FRF ordinate reductions around the single targeted frequency compared to H_2 optimal tuning, while the latter achieves flatter FRFs on a wide frequency range which, arguably, renders it more advantageous for far-field broad-band seismic excitation. Further, Figure 6b plots similar results for the case of a ViBa with $m_{IViBa} = m$. Whilst ViBa is slightly more efficient to control resonant harmonic excitation, the IViBa achieves better overall suppression of the FRF ordinates at a wide range of frequencies for both H_∞ and H_2 tuning.

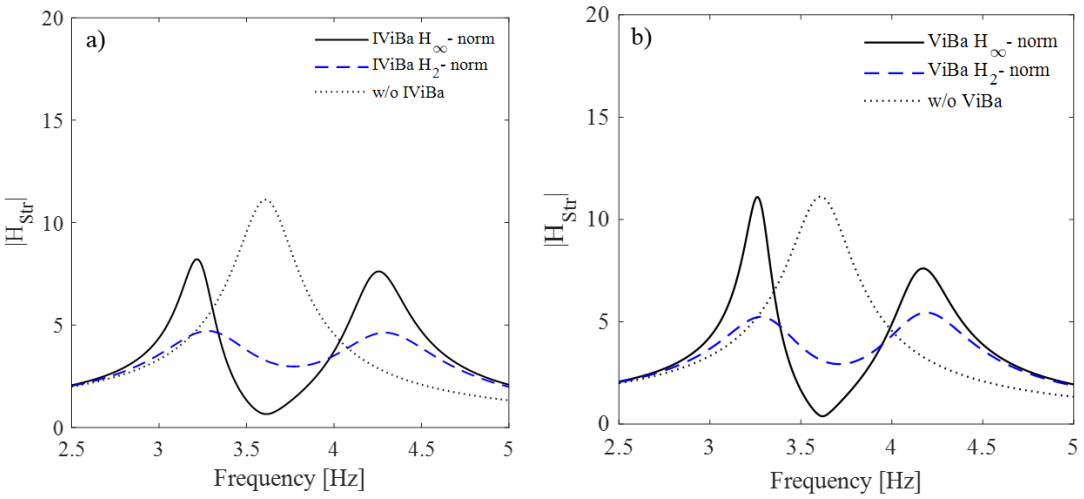

Figure 6 Effect of different optimal tuning approaches to the $H_{str}(\omega)$ FRFs for a) IViBa with $m_{IViBa} = m$ and $b = 1.5m$, b) ViBa with $m_{IViBa} = m$.

In order to quantify the reduction of structural response to broadband/earthquake excitations, the following reduction factor (RF) index is defined

$$RF = \frac{\int_0^{\omega_{cut}} H_{str}^*(\omega) H_{str}(\omega) d\omega}{\int_0^{\omega_{cut}} H_{str,unc}^*(\omega) H_{str,unc}(\omega) d\omega} \tag{12}$$

where $H_{str,unc}$ is the transfer function of the uncontrolled SDOF structure structural response without the protection of the IViBa or ViBa (i.e. uncoupled system). Clearly, smaller RF values entails better (I)ViBa displacement suppression performance to broadband seismic excitations. Figure 7a plots RF as a function of the inertance for (I)ViBa optimally designed in the H_∞ and H_2 sense for $m_{IViBa} = m$. Expectedly, H_2 optimization yields smaller RF values since it involves the minimization of an objective function similar to the definition of the RF in Equation 12. It is further seen that performance improvement saturates as the inertance increases for both optimal design approaches: this trend is in alignment with trends observed in coupling a TMD with a grounded inerter (see Marian and Giaralis 2014 and 2017).

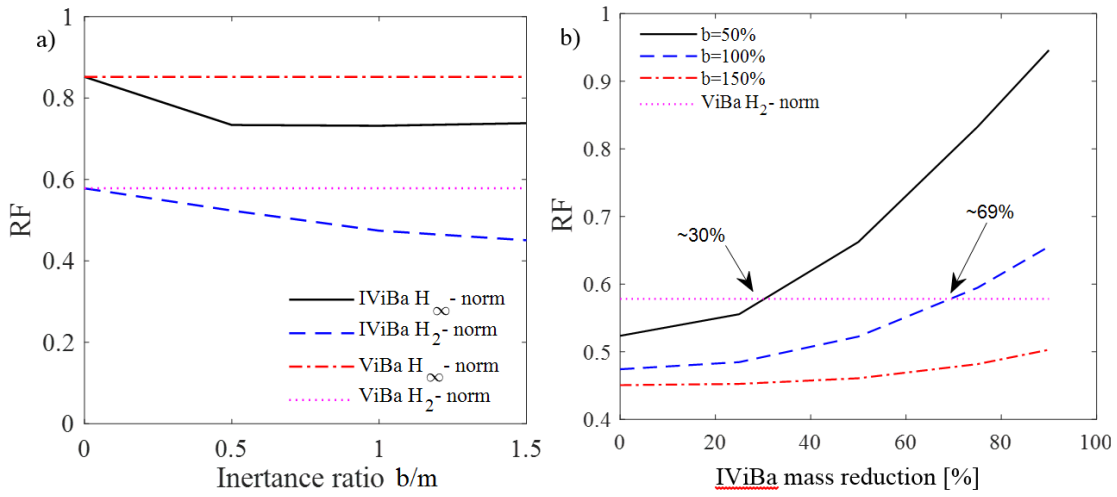

Figure 7. Reduction factor in Equation 12 of (I)ViBa a) for different optimal design approaches, and b) for different values of inertance.

More importantly, Figure 7b plots RF curves for H_2 optimal tuning as function of m_{IViBa} reduction ranging from $m_{IViBa} = m$, i.e. mass reduction equal to 0%, to $m_{IViBa} = 0.1m$, i.e. mass reduction equal to 90% and for fixed inertance. The constant RF value of 0.58 obtained by H_2 optimal ViBa tuning for $m_{ViBa} = m$ is indicated on the figure. Firstly, it is noted that for large inertance, $b = 1.5m$ the efficiency of the IViBa for RF reduction is insignificantly influence by the m_{IViBa} mass. Therefore, more dramatic mass/weight reduction is achieved for smaller inertance values. Secondly, significant mass/weight reduction for a fixed performance RF is achieved by the inclusion of the grounded inerter to the ViBa. For quantification, the mass reduction achieved by IViBa with inertance $b = 0.5m$ and $b = m$ for the same RF yielded by a ViBa with $m_{ViBa} = m$ are noted (at intersections between RF=0.58 threshold with the RF curves): Incorporation of a grounded inerter with $b = 0.5m$ and optimal H_2 tuning reduces the required ViBa mass for the same performance by 30%. Increasing the inertance to b=m achieves mass reduction of about 69% for the same performance.

4.5 Time-domain performance of optimal IViBa design for quasi-stationary base excitation

The previously quantified ViBa mass reduction/replacement effect of the grounded inerter is herein

appraised by undertaken response history analyses to an artificial quasi-stationary accelerogram. The acceleration trace of the excitation, $\ddot{u}_g(t)$, is plotted in Figure 8a. It is a time-enveloped realization of a zero-mean stationary Gaussian stochastic process defined in the frequency domain by a one-sided power spectral density (PSD) function shown in Figure 8b (see e.g., Giaralis and Spanos 2009). The PSD is modelled by the Clough-Penzien (1975) spectrum given as

$$PSD(\omega) = \frac{\omega_g^4 + 4\zeta_g^2\omega^2\omega_g^2}{\left(\omega_g^2 - \omega^2\right)^2 + 4\zeta_g^2\omega_g^2\omega^2} \frac{\omega^4}{\left(\omega_f^2 - \omega^2\right)^2 + 4\zeta_f^2\omega_f^2\omega^2} \tag{13}$$

with parameters $\omega_g = 23$ rad/s, $\omega_f = 2.3$ rad/s, $\zeta_g = 0.6$, and $\zeta_f = 0.6$.

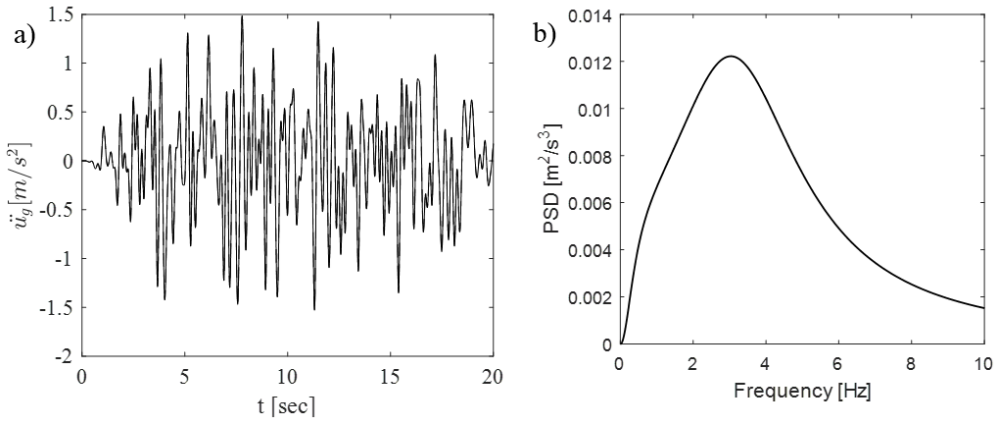

Figure 8 Quasi-stationary seismic excitation: a) time-domain trace and b) Power spectral density function

Figure 9 plots displacement response time histories of the SDOF structure in Figure 1 relative to the ground, $u_{rel}(t)$, for the three optimal H_2 (I)ViBa cases discussed in Figure7b having the same performance corresponding to RF=0.58 for the accelerogram in Figure 8a. The relative response displacement of the uncontrolled structure to the same accelerogram is superposed. It is verified that all three different (I)ViBa designs achieve the same peak response reduction with respect to the uncontrolled structure of about 30%. This finding verifies numerically the potential of the grounded

inerter in the proposed IViBa configuration in Figure 1 to reduce the required ViBa mass in achieving the same level of oscillatory motion reduction of structures.

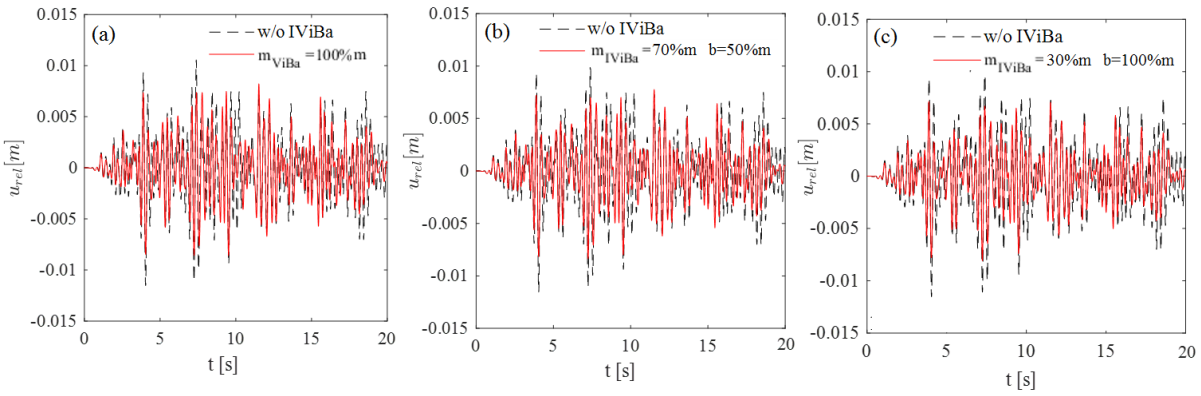

Figure 9 Time history of relative to the ground structural response displacement for SDOF structures protected by a) ViBa, b) IViBa with b=0.5m and $m_{IViBa} = 0.7m$, and c) IViBa with b=m and $m_{IViBa} = 0.3m$.

5. CONCLUDING REMARKS

The ViBa has been coupled with a grounded inerter acting as a mass amplifier to reduce the required ViBa mass/weight while maintaining a desired level of vibration suppression. In this setting, the potential of the resulting IViBa configuration has been explored to mitigate the displacement of an adjacent structure modelled as a SDOF oscillator subjected to either harmonic or broad-band ground excitation. For the case of harmonic excitation, optimal IViBa tuning/design formulae have been derived in closed form to minimize resonant SDOF oscillator response in the H_∞ sense. For the case of broad-band (i.e., clipped white noise) excitation, optimal IViBa stiffness and damping properties have been derived numerically to minimize the RMS SDOF displacement response (H_2 optimal control). In the numerical part of the work adopting properties extracted from a small-scale ViBa prototype specimen, response displacement reductions compared to the uncontrolled SDOF structure of over 90% for harmonic vibrations and of about 30% in case of broadband ground excitation have been noted for

the IViBa. A comparison between ViBa and IViBa showed that the same level of vibration control under earthquake-induced broadband excitations can be achieved by H_2 optimal tuning of IViBa with 70% smaller mass compared to a ViBa if an appropriate value of inertance is adopted. This has been ascertained through response history analyses for an artificial non-stationary accelerogram compatible with a quasi-stationary stochastic seismic acceleration process. Overall, the herein furnished numerical data indicate that coupling the ViBa with a grounded inerter is a bona fide solution to achieve non-invasive seismic protection of structures as a significant lower excavation and material usage cost. Still, further computational as well as experimental work is warranted to address multi-degree-of-freedom structures with exhibiting possibly inelastic behavior and more refined methods to represent the earthquake input action including far-field and near-field recorded accelerograms. The authors are currently undertaking research along the above lines.

7. REFERENCES

Avramidis I, Athanatopoulou A, Morfidis K, Sextos A, Giaralis A (2016). Eurocode-compliant seismic analysis and design of r/c buildings: Concepts, commentary and worked examples with flowcharts, Springer International Publishing, Switzerland.

Cacciola P, Tombari A (2015). Vibrating barrier: a novel device for the passive control of structures under ground motion. *Proceedings of the Royal Society, A*, 471: 20150075.

Cacciola P, Garcia Espinosa M, Tombari A (2015). Vibration control of piled-structures through structure-soil-structure-interaction. *Soil Dynamics and Earthquake Engineering*, 77: 47-57.

Cacciola P, Banjanac N, Tombari A (2017). Vibration Control of an existing building through the Vibrating Barrier. *Procedia Engineering*, 199: 1598–1603.

Clough RW, Penzien J (1993). Dynamics of Structures, 2nd ed., McGraw-Hill Book Company, New York.

Coronado JD, Lomurno R, Tombari A, Cacciola P (2017). Improving Urban Seismic Resilience through Vibrating Barriers. *Proceedings of the 12th ICOSSAR International Conference on Structural Safety and Reliability for Integrating Structural Analysis, Risk and Reliability*, 6-10 August, Vienna, Austria.

Giaralis A, Spanos PD (2009). Wavelets based response spectrum compatible synthesis of accelerograms-Eurocode application (EC8). *Soil Dynamics and Earthquake Engineering*, 29: 219-235.

Giaralis, A., and Petrini, F. (2017). Wind-Induced Vibration Mitigation in Tall Buildings Using the Tuned Mass-Damper-Inerter. *Journal of Structural Engineering, ASCE,* 143: 04017127.

Giaralis A, Taflanidis A (2018). Optimal tuned mass-damper-inerter (TMDI) design for seismically excited MDOF structures with model uncertainties based on reliability criteria. *Structural Control and Health Monitoring*, 25(2): e2082.

Marian L, Giaralis A (2014). Optimal design of a novel tuned mass-damper–inerter (TMDI) passive vibration control configuration for stochastically support-excited structural systems. *Probabilistic Engineering Mechanics* 38, 156–164.

Marian L, Giaralis A (2017). The tuned mass-damper-inerter for harmonic vibrations suppression, attached mass reduction, and energy harvesting. *Smart Structures and Systems* 19, 665–678.

Naeim F, Kelly JM (1999). Design of seismic isolated structures: From theory to practice. Wiley & Sons, Chicester.

Papageorgiou C, Smith MC (2005). Laboratory experimental testing of inerters. (IEEE), pp. 3351–3356.

Smith MC (2002). Synthesis of mechanical networks: the inerter. *IEEE Transactions on Automatic Control*, 47: 1648–1662.

Soong TT, Dargush GF (1997). Passive energy dissipation systems in structural engineering. Wiley & Sons, Chichester.

Tombari A, Zentner I, Cacciola P (2016). Sensitivity of the stochastic response of structures coupled with vibrating barriers. *Probabilistic Engineering Mechanics*, 44: 183–193.

Tombari A, Garcia Espinosa M, Alexander NA, Cacciola P (2018). Vibration control of a cluster of buildings through the Vibrating Barrier. *Mechanical Systems and Signal Processing*, 101: 219–236.

Toscano R (2013). Structured controllers for uncertain systems: a stochastic optimization approach, Springer, New York.

Watanabe Y, Ikago K, Inoue N, Kida H, Nakaminami S, Tanaka H, Sugimura Y, Saito K (2012). Full-scale dynamic tests and analytical verification of a force-restricted tuned viscous mass damper, *Proceedings of the 15th World Conference on Earthquake Engineering*, 24-28 September, Lisbon, Portugal, Paper ID #1206.

Zuo L (2009). Effective and Robust Vibration Control Using Series Multiple Tuned-Mass Dampers. *Journal of Vibration and Acoustics*, 131: 031003.